Volume 23
Number 7
March 28, 1984

Inorganic Chemistry

© Copyright 1984 by the American Chemical Society

Articles

Contribution from the Department of Inorganic Chemistry, University of Marburg, D-3550 Marburg 1, West Germany

Cu^{2+} in 5-Coordination: A Case of a Second-Order Jahn–Teller Effect. 2. $CuCl_5^{3-}$ and Other $Cu^{II}L_5$ Complexes: Trigonal Bipyramid or Square Pyramid?

D. REINEN* and C. FRIEBEL

Received May 18, 1983

The results of single-crystal EPR studies and other spectroscopic measurements on $[Co(NH_3)_6]CuCl_5$ at low temperatures give evidence that the apparent compressed $CuCl_5$ trigonal bipyramid at 298 K is the dynamic average over elongated square pyramids, which are frozen out in the low-temperature phase. Experimental data on $CuCl_5^{3-}$ and various other systems with isolated CuL_6 polyhedra are in accord with a slight energetic preference of an elongated SP with respect to a compressed TBP for d^9 cations. This finding is rationalized in terms of a second-order Jahn–Teller effect and the angular-overlap model. The interrelation of electronic effects on the one hand and geometric packing and steric ligand effects on the other hand in determining the geometries of 5-coordinate Cu^{2+} complexes is finally considered.

Introduction

Electrostatic calculations[1] for ML_5 compounds give evidence that a trigonal bipyramid (TBP) with larger axial than equatorial M–L bond lengths is energetically slightly preferred with respect to a square pyramid (SP) in which the equatorial M–L bonds are longer than the apical bond distance. This result is supported by the available experimental data, if one restricts to examples where additional electronic effects are absent. In most cases trigonal bipyramids are found, but some coordination polyhedra with intermediate geometries are also known.[1] The influence of electronic effects is obvious, if a lone pair of electrons is present. In general a square-pyramidal geometry is stabilized in those cases—as is well known.[2] It is also worthwhile, however, to consider the effect of d electrons on the interplay between the two coordination alternatives. We discuss the d^9 case of Cu^{2+} explicitly here. In order to inform oneself about the d contributions to the respective stabilization energies, it is first necessary to consider Cu^{2+} in a ligand field of five equal ligands with the additional condition that the polyhedra exist isolated from each other in the unit cell. Interconnections or the presence of different and/or polydentate ligands will impose strains on the polyhedra and mislead the arguments. The $CuCl_5^{3-}$ entity in various compounds, which we have investigated by various spectroscopic methods, will be the main subject of discussion. The problem is rather complex, however, because structural data at 298 K often may not reflect the stable coordination geometry, but rather may represent the dynamical average over several static conformations of a different symmetry. We will also consider this aspect here.

Experimental Section

The preparation of the investigated compounds always followed the procedures in the referenced papers. The reflection spectra were recorded by a Zeiss PMQ II spectrophotometer (Infrasil) with a low-temperature attachment. We used Sr_2ZnTeO_6 (4000–12 000 cm^{-1}) and freshly sintered MgO (8000–30 000 cm^{-1}) as standards.

The EPR spectra were taken with an E15-Varian spectrometer (X- and Q-band frequencies) and DPPH as internal standard ($g = 2.003_7$). A variable-temperature accessory (120–400 K) and low-temperature equipment (4.2 K) were available.

The IR-Fourier and Raman measurements were performed in the Max-Planck-Institut für Festkörperchemie, Stuttgart and Anorganisch-Chemisches Institut, Universität Kiel, respectively.

Results and Discussion

$Cu^{II}L_5$ Polyhedra

$Cu^{II}L_5$ polyhedra with $L \equiv NH_3$, Cl^-, and Br^- represent the few examples of 5-coordinated complexes that fulfill the conditions given in the Introduction. A structure determination of $K[Cu(NH_3)_5](PF_6)_3$[3] and EPR data for this and the various other compounds $Cu(NH_3)_5X_2$ with different X[4] are indicative for a nearly square-pyramidal arrangement of ligands. The X-ray evidence[3] places the Cu^{2+} ion above the equatorial plane toward the apical ligand and induces deviations of the bond angles from 90° (α) and 180° (β) (Figure 1, Table I). An additional important structural feature is the much larger apical compared to the equatorial bond lengths, which is reminiscent of the tetragonal elongation of octahedral Cu^{2+}

(1) D. L. Kepert in "Inorganic Chemistry Concepts", Vol. 6, Springer-Verlag, New York, 1982, p 36.
(2) R. J. Gillespie and R. S. Nyholm, *Q. Rev. Chem. Soc.*, **11**, 339 (1957); J. S. Wood, *Prog. Inorg. Chem.*, **16**, 227 (1972).
(3) M. Duggan, N. Ray, and B. J. Hathaway, *J. Chem. Soc., Dalton Trans.*, 1342 (1980).
(4) A. A. G. Tomlinson and B. J. Hathaway, *J. Chem. Soc. A*, 1905 (1968).

0020-1669/84/1323-0791$01.50/0 © 1984 American Chemical Society

Table I. Coordination Geometry of CuL_5 Polyhedra [L = Cl, N Ligator Atoms; Bond Angles (deg) and Bond Lengths (Å) Defined in Figure 1; Deviations from Average Values in Parentheses]

geometry or ligands	$\alpha_{1,3}$	$\alpha_{2,4}$	β_1	β_2	a_1	a_2	a_5	ref
TBP	90	120	180	120		$=a_5$	$=a_2$	
SP[a]	$\gtrsim$90		$\lesssim$180		$=a_2$	$=a_1$		
5 Cl[b]	90	120	180	120	2.29	2.39		9
	$\gtrsim$90		$\lesssim$180		$\simeq$2.29		$\simeq$2.59	this study
	97.$_5$ (3)		165		2.31$_5$ (2$_5$)		2.57	17
5 NH_3	97.$_5$		165 (1)		2.03 (2)		2.19$_5$	3
tren, NH_3	90 (5)	119	180	119	2.03 (2)	2.08		3
tren, NCS	90 (6)	114	178	129.$_5$	1.99$_5$ (4)[c]	2.05$_5$	2.14$_5$	29
2 bpy, NH_3	89 (9)	115 (7)	176	129.$_5$	1.97 (1)	2.06 (1)	2.11	35
2 bpy, NCS	89 (9)	111 (6.$_5$)	175	138	1.98$_5$ (1)	2.02 (5)[c]	2.12	36

[a] C_{4v} symmetry, with Cu^{2+} above the equatorial plane. [b] $[Co(NH_3)_6]CuCl_5$ high-temperature phase, $[Co(NH_3)_6]CuCl_5$ low-temperature phase, and $[N$-(2amet)pipz$H_3]CuCl_5$ (298 K data) are given by lines 1, 2, and 3, respectively. [c] Large deviations because of the short Cu–NCS bond with respect to the other Cu–N spacings.

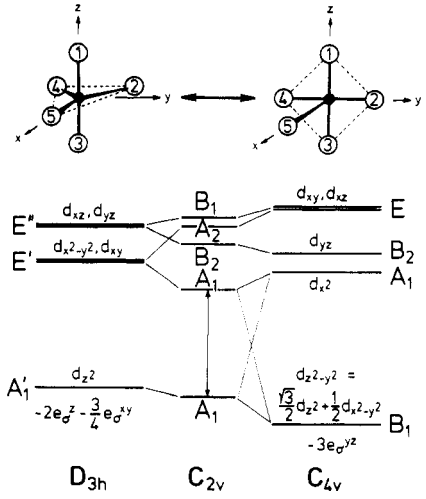

Figure 1. Energy level diagrams of Cu^{2+} in ligand fields of D_{3h} (TBP), C_{4v} (SP), and intermediate C_{2v} symmetry. The respective CuL_5 coordination geometries [$\angle L_5CuL_i \equiv \alpha_i$, $\angle L_{1(2)}CuL_{3(4)} \equiv \beta_{1(2)}$; $d(Cu-L_{1,3}) \equiv a_1$, $d(Cu-L_{2,4}) \equiv a_2$, $d(Cu-L_5) \equiv a_5$] and the AOM energies of the ground states are also given.

complexes as the consequence of a first-order Jahn–Teller effect.[5] The observation of an elongated SP is clearly in contradiction to the electrostatic calculations. Figure 1 gives the energy level diagrams for the alternative C_{4v} and D_{3h} geometries, interconnected by a common reference coordinate system in the sense of a Berry rotation. While the TBP demands a d_{z^2} ground state with a **g** tensor

$$g_z = g_\parallel = g_0 - 3(u_\parallel{}^2 + u_\perp{}^2 - u_\parallel u_\perp)$$
$$g_x = g_y = g_\perp = g_0 + 6u_\perp - 6u_\perp{}^2 \quad (1)$$

the SP ($d_{z^2-y^2}$ ground state) induces the g parameters

$$g_x = g_\parallel = g_0 + 8u_\parallel - 3u_\perp{}^2 - 4u_\parallel u_\perp$$
$$g_y = g_z = g_\perp = g_0 + 2u_\perp - 4u_\parallel{}^2 \quad (2)$$

Third-order orbital contributions are included. The u_i's are defined by (compare Figure 1)

$$u_i = k_i{}^2\lambda_0/\Delta_i \quad (i = \parallel, \perp) \quad (3)$$

with $\Delta_\parallel = E(B_2) - E(B_1)$ and $\Delta_\perp = E(E) - E(B_1)$ for C_{4v} and $\Delta_\parallel = E(E') - E(A_1')$ and $\Delta_\perp = E(E'') - E(A_1')$ for D_{3h}. Obviously EPR spectroscopy is the method of choice to distinguish between trigonal-bipyramidal and square-pyramidal geometries that induce **g** tensors $g_\perp > g_\parallel \simeq g_0$ and $g_\parallel > g_\perp > g_0$, respectively. The four $Cu(NH_3)_5{}^{2+}$ polyhedra in the unit cell of $K[Cu(NH_3)_5](PF_6)_3$ have parallel or antiparallel orientations of the apical Cu–N bond lengths[3] ("ferrodistortive order").[5] Hence, the **g** tensor reflects the molecular geometry, even if exchange coupling is present (see below). The experimental g values of the mentioned compound and other complexes with $Cu(NH_3)_5{}^{2+}$ cations [$g_\parallel = 2.26$ (2), $g_\perp = 2.06$ (1)][3,4] are clearly in accord with a C_{4v} symmetry. The EPR spectra are anisotropic only at low temperatures and become isotropic somewhat below or above 300 K—presumably induced by a complete Berry pseudorotation of the $Cu(NH_3)_5{}^{2+}$ entities in the respective lattice, which leads to symmetry-equivalent axial and equatorial bond lengths in the dynamic average. The ligand field spectra[4] exhibit an absorption maximum at about 15 000 cm^{-1} with a distinct shoulder around 11 000 cm^{-1}, which may be tentatively assigned to the $B_1 \rightarrow B_2$, E and $B_1 \rightarrow A_1$ transitions, respectively. All mentioned transitions are symmetry allowed, if LS coupling is included. The covalency parameters $k_\parallel \simeq k_\perp \simeq 0.75$ as derived from eq 3 are consistent with data for Cu–N bonds in various other compounds.

If the CuN_5 polyhedra do not constitute isolated entities in the unit cell but are connected to the lattice frame by common corners or edges for example, changes in the local geometry may occur. A well-known case is the trigonal bipyramid $[Cu(NH_3)_2(NCS)_3]^-$ in $Cu(NH_3)_2Ag(SCN)_3$.[6] The lattice contains regular AgS_6 octahedra, which are linked by Cu^{2+}. This linkage obviously forces a trigonal planar coordination of NCS^- anions around the Cu^{2+} ions, with short equatorial Cu–N bonds (1.92 Å). Two axial NH_3 ligands (2.00 Å) complete a trigonally elongated TBP. The **g** tensor obeys eq 1 down to 4 K and hence confirms the nonfluxional geometry of the CuN_5 polyhedra.

In apparent contrast to the results reported for isolated $Cu(NH_3)_5{}^{2+}$ entities, room-temperature X-ray structure analyses of $[T^{III}(NH_3)_6]CuCl_5$ (T^{III} = Cr,[8] Co;[9] space group $Fd3c$) reveal $CuCl_5$ polyhedra of perfect trigonal-bipyramidal geometry. The axial bond lengths are shorter than the equatorial ones (Table I), however, which is in disagreement with the electrostatic predictions.[1,2] A second striking feature is the strongly anomalous temperature ellipsoids of the equatorial chlorine ligands, the long axes of which are oriented perpendicular to the Cu–L bonds but inclined with respect to the equatorial plane. The existence of a first-order phase transition at T_c = 280.8 K has been established for $[Co(NH_3)_6]CuCl_5$ by thermochemical measurements[10]—in accord

(5) D. Reinen and C. Friebel, *Struct. Bonding (Berlin)*, **37**, 1 (1979).
(6) H. Jin-ling, L. Jien-ming, and L. Jia-xi, *Hua Hsuek Hsueh Pao* **32**, 194 (1966).
(7) S. Tyagi, B. J. Hathaway, S. Kremer, H. Stratemeier, and D. Reinen, *J. Chem. Soc., Dalton Trans.*, in press.
(8) K. N. Raymond, D. W. Meek, and J. A. Ibers, *Inorg. Chem.*, **7**, 1111 (1968).
(9) I. Bernal, J. D. Korp, E. O. Schlemper, and M. S. Hussain, *Polyhedron*, **1**, 365 (1982).
(10) E. F. Epstein, I. Bernal, and W. P. Brennan, *Inorg. Chim. Acta*, **20**, L47 (1976).

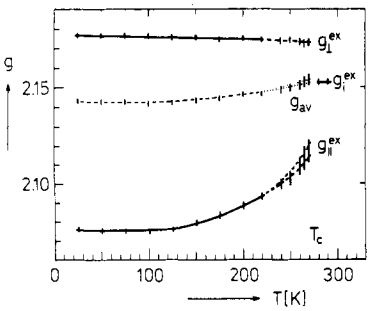

Figure 2. Temperature dependence of the g parameters of $[Co(NH_3)_6]CuCl_5$ (from EPR powder data at 9.5 GHz). The $g_\parallel^{ex}$ components are only badly resolved between 240 K and T_c and could not be determined exactly. Calculated averaged g values below T_c are also shown.

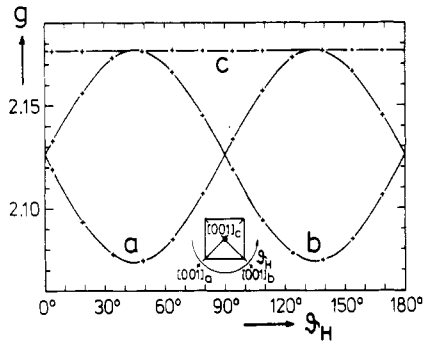

Figure 3. Angular dependence of the **g** tensor of a $[Co(NH_3)_6]CuCl_5$ single crystal with octahedral shape and the indicated orientation at 120 K [three domains a, b, and c with the relative intensities 5:2:1. The orientations of the domains with respect to the magnetic field are $\perp$[001], $\perp$[010], and $\perp$[100] (cf. Figure 4).

with EPR powder investigations that yielded an isotropic signal at 298 K and a tetragonal **g** tensor at 77 K.[11] We have studied the EPR powder spectra in the temperature range between 300 and 4 K. The **g** tensor changes from cubic to tetragonal at $T_c \simeq 280$ K (Figures 2 and 6). Though the phase transition appears also to be of first order for the **g** tensor as order parameter, the g anisotropy still increases considerably with decreasing temperature below T_c and reaches its final value only at 120 K ($g_\parallel^{ex} = 2.07_5$, $g_\perp^{ex} = 2.17_7$). At this temperature we have measured the angular g dependence of a single crystal. The cooling procedure from 298 K to temperatures below T_c has lead to extensive twinning and hence to a three-domain pattern in the EPR spectra (Figure 3). The intensities of the three signals vary strongly, depending on the preparation and cooling conditions. The observation of only one **g** tensor for each domain, which obeys the relation $g_\perp > g_\parallel > g_0$, is strongly indicative of exchange coupling.[5] In this paper we describe a model that explains the symmetry and angular dependence of the **g** tensor and the magnitude of the g values in a consistent manner.[12]

In the low-temperature phase the $CuCl_5$ polyhedra are (possibly slightly distorted) tetragonal pyramids with orientations of the apical bond directions as depicted in Figure 4. Referring to one-eighth of the unit cell of the high-temperature phase, four Cu^{2+} polyhedra are present. They constitute two pairs, which are distinguished by an alignment of the apical bond in opposite directions. Every pair (Cu–Cu spacing $\simeq$ 7.8 Å) corresponds to square pyramids with a perpendicular orientation of the apical bonds (canting angle $2\gamma \simeq 90°$; "antiferrodistortive" order pattern).[5] If these two sublattices

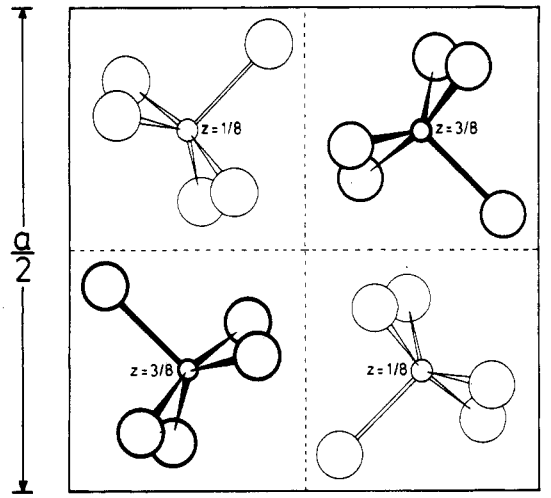

Figure 4. Arrangement of (distorted) $CuCl_5^{3-}$ square pyramids in the tetragonal low-temperature structure of $[Co(NH_3)_6]CuCl_5$ as proposed from EPR data (one-eighth of the unit cell at 298 K; antiferrodistortive order[5] of elongated square pyramids).

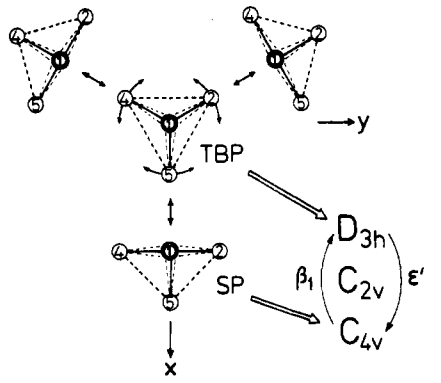

Figure 5. Pathway of pseudorotation between square-pyramidal conformations via a trigonal bipyramid (the apparent $CuCl_5^{3-}$ TBP in $[Co(NH_3)_6]CuCl_5$ as the dynamic average over three SP's). The active vibrational modes for the transitions $D_{3h} \rightleftharpoons C_{4v}$ are also given (cf. Figure 1).

are exchange coupled, a **g** tensor (disregarding third-order contributions)

$$g_\parallel^{ex} = g_\perp = g_0 + 2u_\perp$$
$$g_\perp^{ex} = \tfrac{1}{2}(g_\parallel + g_\perp) = g_0 + 4u_\parallel + u_\perp \qquad (4)$$

is expected (cf. eq 2).[13] If the canting angle deviates from 90°, we obtain a more general relation for $g_\perp^{ex}$, which splits into two components g_1^{ex} and g_2^{ex}:

$$g_1^{ex} = (\cos^2\gamma)g_\parallel + (\sin^2\gamma)g_\perp = g_0 + 2u_\perp + (\cos^2\gamma)(8u_\parallel - 2u_\perp) \quad (5)$$

$$g_2^{ex} = (\sin^2\gamma)g_\parallel + (\cos^2\gamma)g_\perp = g_0 + 2u_\perp + (\sin^2\gamma)(8u_\parallel - 2u_\perp) \quad (6)$$

By eq 4 the molecular **g** tensor $g \simeq 2.28$ and $g_\perp \simeq 2.07_5$ is

(11) R. C. Slade, A. A. G. Tomlinson, B. J. Hathaway, and D. E. Billing, *J. Chem. Soc. A*, 61 (1968).
(12) C. Friebel, to be submitted for publication.
(13) A. Abragam and B. Bleaney, "Electron Paramagnetic Resonance of Transition Ions", Clarendon Press, Oxford, 1970, p 509 ff.
(14) The inclination of the temperature ellipsoids of the equatorial Cl^- ligands with respect to the equatorial plane of the $CuCl_5^{3-}$ TBP in the high-temperature phase[8,9] remains unclear. Possibly a movement of the respective Cl^- ligands perpendicular to this plane superimposes the pseudorotation in Figure 5. This perpendicular component of motion alone would lead to a C_{3v} symmetry with the Cu^{2+} ion above (or below) the equatorial plane of the TBP. Such a geometry, which is indeed observed for CuO_5 polyhedra, may be induced by the preference of d^9 cations for tetrahedral sites.[28] This site preference is even larger for d^{10} cations and could be the reason for the tetrahedral Zn^{2+} coordination in $[Co(NH_3)_6]ZnCl_5$, with a noncoordinated Cl^- ion: D. W. Meek and J. A. Ibers, *Inorg. Chem.*, **9**, 465 (1970).

calculated from the experimental cooperative g values of $[Co(NH_3)_6]CuCl_5$ at 120 K. The sequence $g_\parallel > g_\perp > g_0$ is in accord with eq 2, though the experimental $(g_\parallel - g_0)/(g_\perp - g_0)$ ratio (3.8) is smaller than the usually observed value that is larger than 4. The assumption of a geometry that deviates slightly from a SP toward a TBP (orthorhombic molecular **g** tensor) would remove this inconsistency, however (see below). Long-range magnetic interactions are evident in the EPR spectra at 4 K. An additional spectrum has appeared that is characterized by a considerably larger line width and an orthorhombic $\mathbf{g}^{eff}$ tensor that is spread over a wide magnetic field range (X band: $g_1^{eff} = 3.23$; $g_2^{eff} \simeq 2.20$, $g_3^{eff} = 1.60$). Analogous to Ba_2CuF_6 and K_2CuF_4,[15] the change from g^{ex} to g^{eff} is due to small internal fields, which are induced by ferri- or ferromagnetic coupling of the $CuCl_5^{3-}$ polyhedra.

In our model the phase transition at $T_c \simeq 280$ K is induced by a dynamic process, which is illustrated in Figure 5. The apparent TBP in the high-temperature phase is the dynamic average over three square-pyramidal conformations, the apical bond lengths of which are correlated with the equatorial Cu–Cl distances of the trigonal bipyramid. Two equatorial ligands in the square pyramid are much less affected by the described pseudorotation. They constitute the axial bond lengths of the trigonal bipyramids, which are aligned along the threefold axes of one-eighth of the unit cell (Figure 4). The described model is also in agreement with the anomalous temperature ellipsoids of the equatorial Cu–Cl distances in the trigonal bipyramids,[14] which cannot be explained by rigid-body librations. From the experimental bond lengths, the Cu–Cl distances within the underlying square pyramids can easily be estimated: a(eq) $\simeq 2.29$ Å, a(ap) $\simeq 2.59$ Å (Table I). It remains to explain the isotropic **g** tensor above the phase transition. For the dynamic process of Figure 5, the following molecular g values are calculated from eq 2, if motional narrowing in the EPR spectrum occurs:[16]

$$g_\parallel(\mathrm{dyn}) = g_0 + 2u_\perp \qquad g_\perp(\mathrm{dyn}) = g_0 + 4u_\parallel + u_\perp \quad (7)$$

The presence of exchange interactions, which couple the apparent $CuCl_5^{3-}$ trigonal bipyramids in the cubic unit cell, leads to an isotropic **g** tensor:

$$g_i^{ex} = \tfrac{1}{3}(2g_\perp + g_\parallel) = g_0 + \tfrac{8}{3}u_\parallel + \tfrac{4}{3}u_\perp \quad (8)$$

The decrease in the anisotropy of g^{ex}, if one approaches the phase transition from lower temperatures (Figure 2), can be consistently explained by a change in the geometry of the $CuCl_5^{3-}$ polyhedra. The already slightly distorted square pyramids at $\lesssim 120$ K undergo a further distortion toward the trigonal bipyramid (Figure 5), which becomes larger with increasing temperature (Figure 2). This view is supported by the average **g** tensor, which is 2.14_3 at 25 K $\leq T \leq$ 120 K and increases to 2.15_3 at 280 K—induced by a corresponding shift of the ligand field bands to lower energies (see below). A decrease of the d–d transition energies is indeed expected, if the postulated geometrical changes occur. A more detailed presentation of the EPR results is given elsewhere.[12]

Single-crystal and powder X-ray structure investigations at and below the phase transition are in progress. Powder diffraction patterns in the temperature range from 300 to 12 K have been recorded by a low-temperature Guinier diffractometer and camera. They show a tetragonal splitting of the cubic reflexions below T_c, which increases continuously with decreasing temperature [$a = 15.507$ (1) Å, $c = 22.018$ (2) Å, $c/(2^{1/2}a) = 1.004$ (14 K); presumable space group $I4_1/acd$].

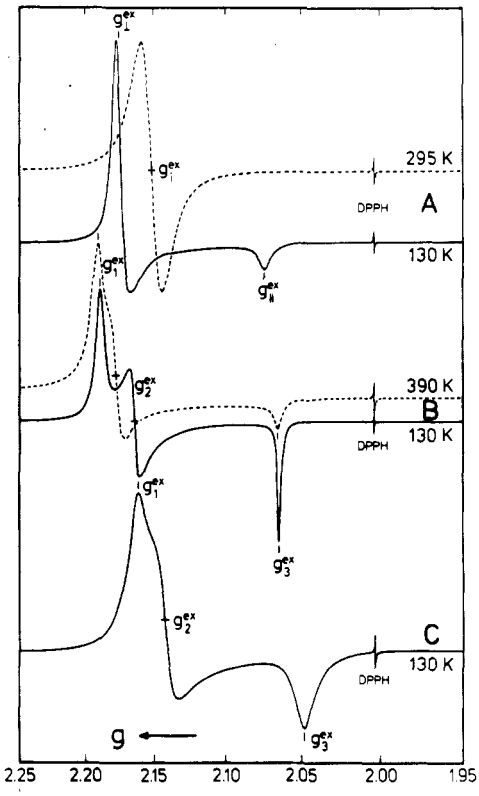

Figure 6. EPR powder spectra of $[Co(NH_3)_6]CuCl_5$ (A), [*N*-(2amet)pipzH_3]$CuCl_5$ (B), and [dien H_3]$CuCl_5$ (C) (35 GHz with DPPH as internal standard).

A tetragonal unit cell of the low-temperature phase is indeed in accord with our model (Figure 4), though the extent of distortion is only very small. This is not unexpected, because our model implies a considerable change of the molecular $CuCl_5^{3-}$ geometry but not necessarily a stronger influence on the unit cell dimensions. No further phase transition is found below T_c and 12 K. A full account of the structural results will be given after completion.[17]

Further support for the model comes from the results of a recent crystal structure determination of *N*-(2-ammonioethyl)piperazinium pentachlorocuprate(II) dihydrate.[18] The monoclinic unit cell (space group $P2_1/a$) contains four $CuCl_5^{3-}$ polyhedra with nearly regular square-pyramidal geometry (Table I), in which the apical bond direction deviates slightly from the normal to the equatorial plane. The four polyhedra correspond to four sublattices with relative orientations similar to those proposed for the low-temperature structure of $[T^{III}(NH_3)_6]CuCl_5$. Only the canting angle, which characterizes the two "antiferrodistortive pairs" (Cu–Cu spacing 7.4 Å), deviates somewhat from the ideal value of 90° (see below). The presence of only one signal in a single-crystal EPR experiment is indicative of exchange coupling in this case also. The measured **g** tensor is orthorhombic [$g_3^{ex} = 2.06_5$, $g_2^{ex} = 2.17_1$, $g_1^{ex} = 2.18_9$ (298 K); $g_{av} = 2.14_1$]. Changing the temperature affects only g_2^{ex} [2.17_6 (390 K); 2.16_4 (130 K)] significantly (Figure 6). On the assumption of regular C_{4v} geometry for the $CuCl_5$ square pyramids and utilization of eq 9, which results from eq 4–6, canting angles $2\gamma \simeq 86°$ (298

$$\cos(2\gamma) = (g_1^{ex} - g_2^{ex})/(g_1^{ex} + g_2^{ex} - 2g_3^{ex}) \quad (9)$$

K) and 84° (130 K) are obtained[19]—in close agreement with the crystallographic value of $2\gamma' = 83.5°$. The molecular g

(15) C. Friebel, V. Propach, and D. Reinen, *Z. Naturforsch., B: Anorg. Chem., Org. Chem.*, **31B**, 1574 (1976); D. Reinen and S. Krause, *Inorg. Chem.*, **20**, 2750 (1981).

(16) The g values are identical with those in eq 4, though the causing effects are different—exchange coupling and dynamic averaging, respectively.

(17) W. Abriel, W. Appel, H. Oelkrug, and D. Reinen, to be submitted for publication.

(18) L. Antolini, G. Marcotrigiano, L. Menabue, and G. C. Pellacani, *J. Am. Chem. Soc.*, **102**, 1303 (1980).

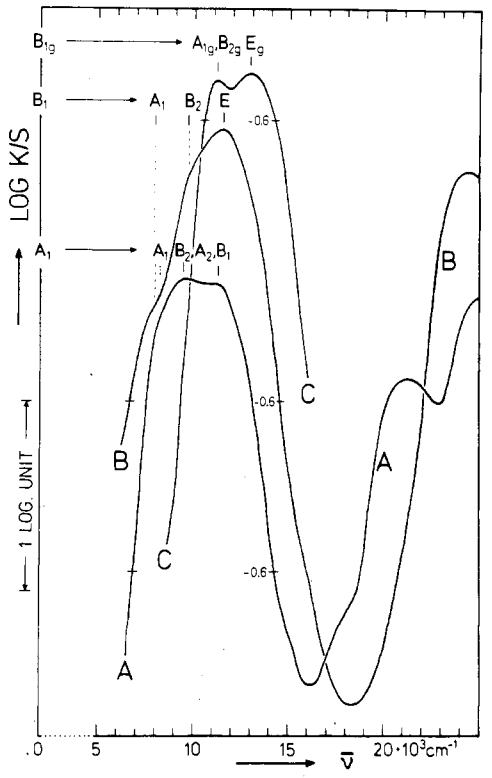

Figure 7. Reflection spectra (5 K) of $[Co(NH_3)_6]CuCl_5$ (A), [*N*-(2amet)pipzH_3]$CuCl_5$ (B), and [dien H_3]$CuCl_5$ (C). Assignments are according to molecular C_{2v} (A), C_{4v} (B), and D_{4h} (C) geometries. Spectra are displaced toward each other with respect to intensities; band maxima occur at 0.95 (A), 0,85 (B), and −0,35 (C) in log (k/s) units. Sr_2TeZnO_6 and dried MgO are standards.

values are estimated to be $g_\parallel \simeq 2.29_5$ and $g_\perp \simeq 2.06_5$, near to those of $[Co(NH_3)_6]CuCl_5$ in the low-temperature phase. The Cu–Cl bond lengths of 2.31$_5$ Å (eq) and 2.57 Å (ap)[18] (Table I) also closely resemble those estimated for low-temperature $[Co(NH_3)_6]CuCl_5$. The succesive substitution of Cl^- by Br^-, which is possible to about 80 mol %, shifts the **g** tensor continuously to significantly lower values: $g_\parallel^{ex} = 2.05_2$, $g_\perp^{ex} \simeq 2.14_4$ ($g_{av} = 2.11_3$).

The 298 K ligand field spectrum of [*N*-(2amet)pipzH_3]-$CuCl_5$ exhibits a broad band that is resolved at 5 K into an intense and asymmetric peak at 11 500 cm^{-1} and a comparatively weak, but distinct, shoulder at 8200 cm^{-1} (Figure 7B). While all d–d transitions are symmetry allowed in C_{4v}, if LS coupling is included, only the $B_1 \rightarrow E$ excitation is allowed without LS coupling. We hence assign this transition to the highest intensity peak. The asymmetry around 10 000 cm^{-1} and the shoulder at 8200 cm^{-1} may then be tentatively correlated with the $B_1 \rightarrow B_2$ and $B_1 \rightarrow A_1$ transitions, respectively. The covalency parameter, calculated from the **g** tensor, is $k = 0.66$ (eq 3). The substitution of Cl^- by Br^- shifts the highest intensity band to slightly higher energies by about 500 cm^{-1}.[18] Hence, the considerable lowering of the g values by the ligand displacement (see above) is mainly due to the expected decrease of the covalency factor k. The low-temperature spectrum of $[Co(NH_3)_6]CuCl_5$ shows a broad absorption band in exactly the same energy region as the compound discussed before, but with a rather different intensity distribution (Figure 7A). We think that a symmetry lower than C_{4v} with a splitting of the tetragonal ^2E state has led to an at least partial overlap of the four possible electronic transitions and thus has induced the intensity changes. This argument of a deviation from a SP toward a TBP (C_{2v} symmetry, Figure 1) was considered above already. There is a striking shift of the d–d transitions in particular in the temperature range around T_c. While at 298 K the peaks of the double bands are observed at 8500 and 10 500 cm^{-1},[20] they move to 9500 and 11 300 cm^{-1} at 5 K. This is in agreement with a corresponding decrease of the g values and was discussed above already. In contrast to our description, the so far reported assignments of the reflection spectra of compounds $[T^{III}(NH_3)_6]CuCl_5$ were based on the assumption of a D_{3h} symmetry.[20]

Comparison of the considered EPR and ligand field data with those of $[(H_3NCH_2CH_2)_2NH_2]CuCl_5$, which does not contain 5-coordinated Cu^{2+}, is also helpful. For the cited compound, planar $CuCl_4^{2-}$ units with slightly anisotropic Cu–Cl spacings of 2.31$_5$ Å (2×) and 2.28 Å (2×) are reported, which are supplemented to strongly elongated octahedra by two axial Cl^- ligands from other planar units in a distance of 2.88 Å.[21] The fifth Cl^- ion is not coordinated to Cu^{2+}. The EPR spectrum is orthorhombic (Figure 6). The **g** tensor ($g_3^{ex} = 2.04_9$, $g_2^{ex} = 2.14_4$, $g_1^{ex} = 2.16_1$; $g_{av} \simeq 2.12$) is exchange narrowed and characteristic for a slightly disturbed antiferrodistortive order. The structure determinations yield four $CuCl_4^{2-}$ planes in the unit cell. They can again be grouped into two pairs, each of which is characterized by an angle of $2\gamma' = 85°$ between the normals to the $CuCl_4^{2-}$ planes[19] and short Cu–Cu distances of about 5 Å. The other Cu–Cu spacings are presumably too large ($\gtrsim$11.8 Å) to induce exchange coupling in the EPR spectra.[22] From the experimental canting angle, molecular g values $g_x = 2.05$, $g_y = 2.05_5$ (1), and $g_z = 2.25$ (1) are calculated (eq 5, but with a splitting of $g_\perp$). They are consistent with the structural data, because a small $g_\perp$ splitting due to the anisotropy in the equatorial Cu–Cl bond lengths may be present. The 5 K ligand field spectrum—in agreement with the 77 K data[20]—reveals a double band at 13 100 and 11 300 cm^{-1}, with the higher energy peak of stronger intensity (Figure 7C). If the two bands are assigned to the transitions $B_{1g} \rightarrow E_g$ and $\rightarrow B_{2g}$, A_{1g} [or $B_{1g} \rightarrow A_{1g}$, E_g and $\rightarrow B_{2g}$] in D_{4h} symmetry, the interpretation is consistent with the spectral results discussed before. The band intensities are about one log (k/s) unit lower than those of the two compounds considered before (Figure 7A,B) and hence in agreement with the presence of an inversion center in this case. The covalency parameter calculated from eq 2 and 3 is $k \simeq 0.64$. The similarity between the energies of the d–d transitions and **g** tensors for [*N*-(2amet)pipzH_3]$CuCl_5$ and $[Co(NH_3)_6]CuCl_5$ on the one hand and the blue-shift of the ligand field spectrum as well as the decrease of the g values for [dienH_3]$CuCl_5$, which is "nearer" to a square-planar coordination, on the other hand gives further support to our model (Figures 6 and 7).

Additional informative results come from the vibrational spectra. Figure 8 shows the drastic changes in the IR spectrum of $[Co(NH_3)_6]CuCl_5$, which occur when the phase transition is passed. The low-temperature spectrum closely resembles the IR spectrum of [*N*-(2amet)pipzH_3]$CuCl_5$[18] (Table II) but shows additional band splittings by a lower symmetry component. This observation is in accord with similar results from the EPR and ligand field spectra. Striking changes are also

(19) Because the $g_\perp$ components of an axial molecular **g** tensor are presumably located in the best equatorial plane, 2γ is defined as the canting angle between the normals to the equatorial planes of two interacting polyhedra, which is not necessarily equal to the canting angle $2\gamma'$ between the long axes of two interacting (slightly distorted) square pyramids.

(20) G. C. Allen and N. S. Hush, *Inorg. Chem.*, **6**, 4 (1967).
(21) T. J. Greenhough and M. F. C. Ladd, *Acta Crystallogr., Sect. B*, **B33**, 1266 (1977), R. Allmann, B. Barucha, and D. Reinen, to be submitted for publication.
(22) W. Henke, S. Kremer, and D. Reinen, *Inorg. Chem.*, **22**, 2858 (1983); T. Rojo, M. Vlasse, and D. Beltranporter, *Acta Crystallogr., Sect. C*, **C39**, 194 (1983); R. Allmann, S. Kremer, and D. Kucharczyk, *Inorg. Chim. Acta*, in press.

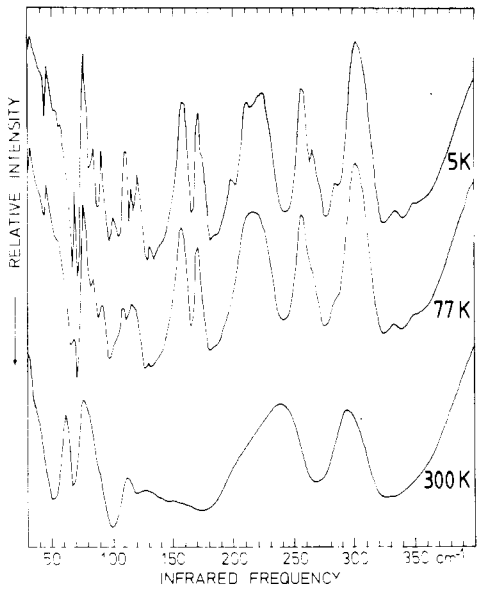

Figure 8. IR Fourier spectra of $[Co(NH_3)_6]CuCl_5$ above (300 K) and below (77 K, 5 K) the phase transition (cf. Table II).

Table II. IR and Raman Data (cm^{-1}) for $[Co(NH_3)_6]CuCl_5$ [Low-Temperature Phase (77 K), I], [*N*-(2amet)pipzH_3]$CuCl_5$ [298 K,[18] II], and [dienH_3]$CuCl_5$ [298 K[24] (77 K Values in Parentheses), III][a]

D_{4h}	I	II	III
A_{1g} (R)	262 vs	265 vs	288 s
E_u (IR)	280[b] s, 242 s	275 vs	292 (298) vs, 266 (270) s
B_{1g} (R)	203 m	214 m	245 s
IR	≃190[c] s	190 vs	210 (217) vs
R	176 s, 168 s	186 s, ≃170 vs	200 w, 180 m
IR	167 m, ≃135[c] s	≃150 s	181 (192, 183) vs, 159 (160) vs, 147 (151) vs

[a] Assignments and selection rules are given for the higher energy bands in D_{4h} symmetry. For I and II the D_{4h} selection rules are slightly relaxed according to the loss of the inversion center [C_{4v}: A_1 and E (R, IR), B_1 (R)]. [b] Split bands and shoulders at 263, 270, 277, and 289 cm^{-1} (Figure 8). [c] Additional band splittings as shown in Figure 8.

observed in the Raman spectrum, if the temperature is lowered. Again, the low-temperature data are very similar to those of [*N*-(2amet)pipzH_3]$CuCl_5$[18] (Table II). Though a complete interpretation of the spectra was not possible for various reasons,[23] the main absorptions in the higher energy region can be assigned to the stretching vibrations of the $CuCl_5^{3-}$ polyhedra. We have chosen the square-planar D_{4h} point group as the approximate local symmetry. The transition to C_{4v}—according to the position of Cu^{2+} a little above the equatorial plane and the presence of a weakly bonded fifth ligand—will then only slightly relax the selection rules connected with the occurrence of an inversion center. The apical ligand in a comparably large bond distance will presumably not give rise to higher energy bands. Above the phase transition the IR spectrum of $[Co(NH_3)_6]CuCl_5$ collapses to a band at 269 cm^{-1} and a broad region of absorption with a maximum at about 175 cm^{-1} and a shoulder around 145 cm^{-1} (Figure 8). Analogously the Raman spectrum reduces to two bands at 259 and 175 cm^{-1}. The 300 K data are in agreement with those of Long et al. and Boormann et al.[24] The reduction in the number of bands on increasing the temperature above T_c is well in accord with the dynamic averaging process (Figure 5) we propose. An assignment of the 300 K spectra according to the apparent D_{3h} symmetry[23] is doubtful, however. The vibrations of [dienH_3]$CuCl_5$ have been included in Table II for comparison. The distinct splitting of the E_u vibration reflects the difference in the equatorial Cu–Cl bond lengths.[21] Again, the similarity with the data of the other two compounds at least in the higher energy region is striking. A significant shift to higher energies is observed, however, because the Cu^{2+} coordination is nearest to a square plane in this case—with the largest energy separation between B_1 and A_1 (Figure 1) and the smallest equatorial Cu–Cl bond lengths.

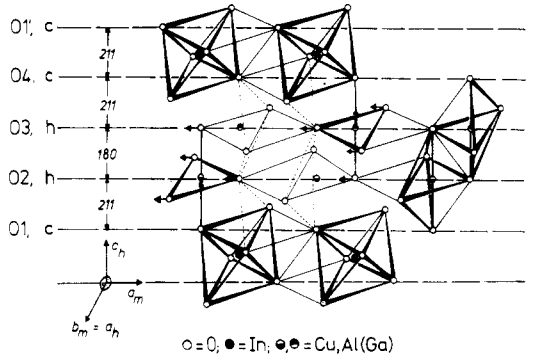

Figure 9. The pseudohexagonal layer structure of $CuAl(Ga)InO_4$[28] with Cu^{2+} and Al^{3+} (Ga^{3+}) in trigonal-bipyramidal coordination. Distances between layers (pm) and orientations of lattice vectors (monoclinic unit cell) are given.

The experimental results and arguments so far give evidence that the stable static geometry of the $CuCl_5^{3-}$ polyhedra in compounds $[T^{III}(NH_3)_6]CuCl_5$ is a square pyramid, in which the apical bond is appreciably longer than the equatorial distances—in analogy to the $Cu(NH_3)_5^{2+}$ polyhedra discussed before. The axially compressed trigonal bipyramid in the high-temperature phase can be understood as the dynamic average of three square-pyramidal conformations, which transform into one another by means of restricted Berry pseudorotations (Figure 5). $[Cr(NH_3)_6]CuBr_5$ is isostructural with the corresponding Cl^- complex with analogous stereochemical properties.[25] Presumably the same dynamic mechanism has to be discussed for this compound also. A short account of the model presented in the preceding section has already been given recently.[26]

Structures with CuO_5 polyhedra are also known. In $KCuPO_4$ half of the Cu^{2+} ions is surrounded by five O^{2-} ligands in a considerably distorted square-pyramidal arrangement, while the other half is tetrahedrally coordinated (compressed along the S_4 axis).[27] The reason for the low site symmetry is presumably that the Cu^{2+} polyhedra are not isolated in the structure but are interconnected by PO_4 tetrahedra. In the compounds $CuAlInO_4$ and $CuGaInO_4$ the 5-coordinated Cu^{2+} (and Al^{3+} or Ga^{3+}) ions are forced into sites with a distorted trigonal-bipyramidal environment by packing effects.[28] The pseudohexagonal compounds contain double layers of trigonal bipyramids, which are connected with each other via common edges (Figure 9). The EPR spectra[28] of Cu^{2+} doped into $MgAl(Ga)InO_4$ are in accord with eq 1 and confirm the trigonal-bipyramidal coordination.

After all, one may conclude that for Cu^{2+} in 5-coordination the tetragonal pyramid with a long apical bond distance is the

(23) D. W. Smith, *Coord. Chem. Rev.*, **21**, 93 (1976).
(24) T. V. Long, A. W. Herlinger, E. F. Epstein, and I. Bernal, *Inorg. Chem.*, **9**, 459 (1970); P. M. Boormann, P. J. Craig, and T. W. Swaddle, *J. Chem. Soc. A*, 2970 (1969).
(25) S. A. Gold field and K. N. Raymond, *Inorg. Chem.* **10**, 2604 (1971).
(26) D. Reinen, Jahn–Teller Conference, Nijmegen, The Netherlands, Sep 1981.
(27) G. L. Shoemaker, E. Kostiner, and J. B. Anderson, *Z. Kristallogr.*, **152**, 317 (1980).
(28) A. Kutoglu, A. Rösler, and D. Reinen, *Z. Anorg. Allg. Chem.*, **456**, 130 (1979); A. Rösler and D. Reinen, *ibid.*, **479**, 119 (1981).

energetically preferred coordination geometry, if the five ligands are identical and if the CuL_5 polyhedra are isolated from each other in the respective structure. On the other hand, it is obviously possible to force Cu^{2+} into a trigonal-bipyramidal coordination, if the polyhedra constitute a rigid interconnected 3-dimensional structure with no opportunity for fluxional behavior in the sense of a Berry mechanism. The existence of $Cu(NH_3)_2Ag(SCN)_3$ and $CuAl(Ga)InO_4$ with CuN_5 and CuO_5 bipyramids demonstrates that the energetic preference of the tetragonal pyramid with respect to the trigonal bipyramid cannot be too distinct.

The energy level diagrams of CuL_5 polyhedra in the alternative D_{3h} and C_{4v} geometries with respect to a common reference coordinate system are given in Figure 1. The group-theoretical analysis shows that a continuous vibrational pathway between the alternative geometries exists (Figure 5), which is conveniently described in terms of a second-order Jahn–Teller effect.[29] The vibrational modes, which induce the transitions from C_{4v} to D_{3h} and vice versa, are of β_1 and ϵ' symmetry, respectively. They lead into intermediate distorted geometries with C_{2v} symmetry, in which configuration interaction is induced between the A_1 ground state and a near-lying excited level of the same symmetry. This interaction lowers and hence stabilizes the ground state. Hence, any limiting or intermediate geometry may be realized, depending on the presence of different kinds of ligands or of ligands that are spacious or multidentate. These factors will be considered in greater detail in the next section. Also the connection pattern within the lattice may have severe stereochemical influence, if the Cu^{2+} polyhedra are involved. Examples have just been discussed. In the case of "isolated" CuL_5 polyhedra with five equal and nonspacious ligands, a (nearly) regular apically elongated square pyramid is the favored coordination geometry with the obviously lowest ground state of all possible conformations. If one refers to the angular-overlap energies, one can easily deduce that the B_1 ground state in C_{4v} symmetry will lower its energy more the shorter the equatorial bond lengths are (increase of e_σ^{yz}, Figure 1). This implies necessarily a considerable apical bond elongation—in perfect agreement with the experimental evidence. The resulting elongated square-pyramidal coordination is strongly reminiscent of the tetragonal elongation, which Cu^{2+} ions in octahedral coordination undergo as the consequence of a first-order Jahn–Teller effect.[5]

Cu^{2+} in 5-Coordination with Multidentate Ligands

The substitution of four NH_3 molecules in $Cu(NH_3)_5^{2+}$ by the tetradentate tren ligand [tris(2-aminoethyl)amine] stabilizes a trigonal-bipyramidal geometry at 298 K in $[Cu(tren)NH_3](ClO_4)_2$, in which NH_3 occupies an axial position.[3] The EPR spectrum is isotropic as the consequence of exchange coupling between the CuN_5 polyhedra, which have orientations analogous to those of the $CuCl_5$ trigonal bipyramids in $[Co(NH_3)_6]CuCl_5$. Structural data are scarce so far,[22] however. This possibly indicates that the TBP represents the energetically preferred static geometry. Some experimental facts are remarkable, however. To begin with, the Cu–N bond lengths in $Cu(tren)NH_3^{2+}$ [2.03 Å (ax), 2.08 Å (eq)][3] are exactly those that would result from those for $Cu(NH_3)_5^{2+}$ [2.03 Å (eq), 2.19 Å (ap)],[3] if the pseudorotation of Figure 5 takes place. Second, the energies of the ligand field bands are nearly identical for $Cu(tren)NH_3^{2+}$ and $Cu(NH_3)_5^{2+}$ [$\simeq$11 000 and $\simeq$15 000 cm^{-1} (298 K)][3]. Only the intensities are essentially different. While the low-energy transition is weak with respect to the high-energy peak for $Cu(NH_3)_5^{2+}$, the reverse situation arises for $Cu(tren)NH_3^{2+}$ [11 800 and 15 500 cm^{-1} (5 K)]. Apparently the energy difference between the alternative D_{3h} and C_{4v} geometries is very low in this case. An axially compressed TBP is indeed energetically favored in D_{3h}. Short axial and long equatorial bond lengths will induce an increase of e_σ^z and a decrease of e_σ^{xy} (Figure 1) and hence stabilize the A_1' ground state ($2e_\sigma^z + {}^3/_4 e_\sigma^{xy} > 0$). The analogous argument in C_{4v} leads to an apical elongation of the square pyramid, as discussed above. A careful analysis of the temperature factors in $[Cu(tren)NH_3](ClO_4)_2$ could presumably give further information. The tren molecule seems to stabilize the TBP because of its specific stereochemical properties. It is an open question, however, whether this tetradentate ligand is also able to adapt the geometry of an elongated SP—necessarily with an occupation of the apical and three equatorial positions. A remarkable example in this connection is the compound [Cu(tren)NCS]SCN at 298 K. The substitution of NH_3 in $Cu(tren)NH_3^{2+}$ by NCS^- (N bonded) leads to an intermediate geometry of the CuN_5 polyhedron. One of the three equatorial Cu–N bond lengths becomes larger (2.14_5 Å) and the other two smaller (2.05_5 Å), while the angle between the shorter bonds surpasses 120° by $9._5$° (Table I).[30] This may be taken again as a proof for the configurational pathway, depicted in Figure 5. The g tensor is orthorhombic (2.08_3, 2.13_2, 2.15_7; $g_{av} = 2.12_4$) and obviously exchange narrowed. The absorption spectrum is nearly identical with the one of $[Cu(tren)NH_3]^{2+}$.[31] While at least an intermediate geometry could be verified by the introduction of the stronger ligand NCS^- instead of NH_3, the trigonal-bipyramidal coordination with g tensors in accord with eq 1 remains, if NH_3 is substituted by weaker ligands such as OH^-, Br^-, and I^-.[3,32] This agrees with our supposition that the energy gain for the square pyramid is essentially accomplished by four short bonds in the equatorial plane. The presence of a weaker ligand in this plane hence destabilizes this geometry.

2,2′,2″-Terpyridine as a tridentate ligand with N ligator atoms is very rigid but can accommodate likewise a (distorted) square pyramid (three equatorial positions) and a (distorted) trigonal pyramid (one equatorial and the two axial positions). Complexes $Cu(terpy)X_2 \cdot nH_2O$ with CuN_3L_2 polyhedra (L = X^-, OH_2) are predominantly square pyramids, which are elongated along one of the Cu–L bond directions,[22] or represent superpositions of the two equivalent square–pyramidal conformations of this geometry. Structural data are scarce so far,[22] however.

Five-coordinate Cu^{2+} complexes with bidentate ligands are numerous, and only some examples will be shortly discussed. The substitution of four NH_3 molecules in $Cu(NH_3)_5^{2+}$ by two "en" ligands preserves the square-pyramidal geometry, presumably with one long apical bond to NH_3. Though crystallographic data are not available, the EPR evidence is unambiguous for most of the compounds $[Cu(NH_3)(en)_2]X_2$ investigated.[33] Particularly interesting are complexes with two 2,2′-bipyridyl ligands $Cu(bpy)_2L$. The spacious and rigid bidentate rings cannot accommodate a strictly square-planar $Cu(bpy)_2^{2+}$ geometry because of intermolecular repulsion. In compounds $[Cu(bpy)_2]X_2$ [$X^- = PF_6^-$ (I), BF_4^- (II), ClO_4^- (III)], for example,[34] a CuN_4 coordination with a dihedral angle of $45._5 \pm 1$° is found, which is supplemented to a strongly elongated "octahedron" by two very weakly bonded F (O) ligands in the axial positions of complex II (III). In I the axial ligands are missing, leaving a 4-coordination, which is rather

(29) R. G. Pearson, *J. Am. Chem. Soc.*, **91**, 4947 (1969).

(30) P. C. Jain and E. C. Lingafelter, *J. Am. Chem. Soc.*, **89**, 6131 (1967).
(31) R. C. Slade, A. A. G. Tomlinson, B. J. Hathaway, and D. E. Billing, *J. Chem. Soc. A*, 61 (1968).
(32) R. Babucci, A. Bencini, and D. Gatteschi, *Inorg. Chem.*, **16**, 2117 (1977).
(33) A. A. G. Tomlinson and B. J. Hathaway, *J. Chem. Soc. A*, 1685 (1968).
(34) J. Foley, S. Tyagi, and B. J. Hathaway, *J. Chem. Soc., Dalton Trans.*, in press; J. Foley, D. Kennefick, D. Phelan, S. Tyagi, and B. J. Hathaway, *ibid.*, 2333 (1983).

a strongly tetragonally compressed tetrahedron than a square plane. Also the rigid bipyridyl ligand cannot occupy two equatorial positions of a TBP because the chelate $N_{1(3)}$–Cu–$N_{2(4)}$ angle is fixed to about 80°. Thus, a TBP, with two N atoms of different bipyridyl molecules in the axial positions, or a SP, in which one bidentate ligand bridges the apical and one equatorial site, is expected to be the preferred geometry, if ligand effects were dominating. The $[Cu(N_1N_2)(N_3N_4)NH_3]^{2+}$ polyhedra in $[Cu(bpy)_2NH_3](BF_4)_2$ with five Cu–N bonds, for example, constitute in first approximation trigonal bipyramids.[35] They are axially compressed, however, due to the electronic effect of the d^9-configurated Cu^{2+} ion because stronger axial and weaker equatorial bonds will lower the energy of the A_1' ground state in D_{3h} symmetry (Figure 1). A closer look into the equatorial plane of the Cu^{2+} polyhedra reveals that the equatorial Cu–N_2 bond length is significantly larger than the other two (Table I). Also the equatorial angle opposite to this bond direction is much larger than 120°. Clearly these geometrical deviations can be understood as a step along the pathway from a compressed TBP to an elongated SP (Figures 1 and 5). The observation of an intermediate coordination geometry is analogous to what has been found for $[Cu(tren)NCS]^+$, discussed above. A more detailed analysis of the Cu–N spacings and NCuN bond angles leads to a model in which an elongation along Cu–N_4—with less statistical weight—superimposes the one along Cu–N_2. An even more pronounced deviation toward a square pyramid is found for the $[Cu(NN)_2NCS]^+$ cation in $[Cu(bpy)_2NCS]BF_4$[36] (Table I). For $[Cu(NN)OH_2]^{2+}$, two interesting alternative cases are found. One ($S_5O_6^{2-}$ as counterion) parallels the examples before—elongation of the Cu–N_2 bond; the other one ($S_2O_6^{2-}$ as anion) implies an elongation along the Cu–O bond direction.[37] The substitution of the weaker ligand Cl^- into the fifth coordination site leads again to compressed trigonal bipyramids, in which also sometimes one equatorial Cu–N bond is distinctly larger, however. The structural profile of CuN_4Cl in various compounds is discussed in detail by Hathaway and co-workers.[38] It is always open to question whether in cases where only structural data at 298 K are available, dynamic averaging effects are present or not. The EPR spectroscopic investigation of some representative examples down to 4.2 K gives evidence, however, that the observed geometry is static.[7]

Concluding, one may state that the geometry of 5-coordinate Cu^{2+} polyhedra with multidentate ligands is determined equally by steric ligand and by electronic effects (Table I). While the former may stabilize—depending on the specific geometry and rigidity of the ligand—any square-pyramidal, trigonal-bipyramidal, or intermediate geometry (Figure 5), the latter always induce the expected bond length anomalies. These are a *compressed* TBP, an *elongated* SP, or any intermediate conformation.[39]

Acknowledgment. We thank W. König, Dr. J. Kuhl, and Prof. A. Simon, Stuttgart, and Dr. H. Homborg and Prof. W. Preetz, Kiel, for the low-temperature IR and Raman spectra, respectively. We further appreciate the discussion with Dr. S. Kremer and the valuable experimental assistance of R. Storch and H. Stratemeier.

Registry No. $[Co(NH_3)_6]CuCl_5$, 16028-79-8; [*N*-(2amet)pipzH_3]$CuCl_5$, 73245-69-9; [dienH_3]$CuCl_5$, 56508-39-5; [Cu(tren)NCS]SCN, 18582-12-2.

(35) F. S. Stephens, *J. Chem. Soc., Dalton Trans.*, 1350 (1972).
(36) S. Tyagi and B. J. Hathaway, *J. Chem. Soc., Dalton Trans.*, 2029 (1981).
(37) D. Harrison and B. J. Hathaway, *Acta Crystallogr., Sect. B*, **B35**, 2910 (1979); D. Harrison, B. J. Hathaway, and D. Kennedy, *ibid.*, **B35**, 2301 (1979).
(38) D. Harrison, D. Kennedy, and B. J. Hathaway, *Inorg. Nucl. Chem. Lett.*, **17**, 87 (1981).
(39) D. Reinen, *Comments Inorg. Chem.*, **2**, 227 (1983).

Contribution from the Department of Chemistry, University of Florence, Florence, Italy

Electronic Structure of the Nitroxyl Complex Bis(di-*tert*-butyl nitroxide)cobalt(II) Bromide

CRISTIANO BENELLI, DANTE GATTESCHI,* and CLAUDIA ZANCHINI

Received July 15, 1983

The magnetic and EPR properties of the nitroxyl complex bis(di-*tert*-butyl nitroxide)cobalt(II) bromide have been reexamined. It is concluded that the ground state is a spin doublet, as shown by the magnetic susceptibility and the EPR spectra at liquid-helium temperature. The *g* values, which show large deviations from the free-electron value, are rationalized in terms of a sum of contributions from the radicals and the high-spin cobalt(II) ion.

Nitroxyl radicals are known to act as weak Lewis bases[1,2] and are widely used as spin probes in biological systems[3-6] and as ligands for a variety of transition-metal ions.[3,7-9] The complexes in which the nitroxyl group is directly bound to the metal ion are of particular interest for the mechanism of coupling of the unpaired electrons of the ligand and of the metal, but not many well-characterized examples are available. The extent of coupling has been found to vary from weak to strong, depending on the relative geometry of the magnetic orbitals of the metal and of the free radical.[2,10-12]

(1) Drago, R. S.; Lim, Y. Y. *J. Am. Chem. Soc.* **1971**, *93*, 891.
(2) (a) Lim, Y. Y.; Drago, R. S. *Inorg. Chem.* **1972**, *11*, 1334. (b) Richman, R. M.; Kuechler, T. C.; Tanner, S. P.; Drago, R. S. *J. Am. Chem. Soc.* **1977**, *99*, 1055. (c) Drago, R. S.; Kuechler, T. C.; Kroeger, M. *Inorg. Chem.* **1979**, *18*, 2337.
(3) Eaton, S. S.; Eaton, G. R. *Coord. Chem. Rev.* **1978**, *26*, 207.
(4) Stone, T. J.; Buckman, T.; Nordio, P. L.; McConnell, H. M. *Proc. Natl. Acad. Sci., U.S.A.* **1965**, *54*, 1010.
(5) Cohn, M.; Reuben, J. *Acc. Chem. Res.* **1971**, *4*, 214.
(6) Berliner, L. J., Ed. "Spin Labelling: Theory and Applications"; Academic Press: New York, 1976.
(7) Volodarski, L. B.; Grigorev, I. A.; Sagdeev, L. Z. *Biol. Magn. Reson.* **1980**, *2*, 169.
(8) Sadgeev, R. Z.; Molin, J. N.; Sadikov, R. A.; Volodarsky, L. B.; Kutikova, G. A. *J. Magn. Reson.* 1973, *9*, 13.
(9) Karayannis, N. M.; Pales, C. M.; Mikulski, C. M.; Pytlewski, L. L.; Blum, H.; Labes, M. M. *Inorg. Chim. Acta* **1973**, *7*, 74.

0020-1669/84/1323-0798$01.50/0 © 1984 American Chemical Society